A ROSSBY-WAVE DYNAMO FOR THE SUN, II*

PETER A. GILMAN

Dept. of Astro-Geophysics, University of Colorado, Boulder, Colo., U.S.A.

(Received 23 January, 1969)

Abstract. To make the analysis more tractable, we simplify the equations of Part I to apply to two superposed layers of fluid, with horizontal variations in the motion and magnetic field represented by a small number of Fourier harmonics. The resulting set of eighteen ordinary nonlinear differential equations in time for the Fourier amplitudes is integrated numerically. We analyze in detail the dynamo action from a typical Rossby wave motion and compare it with the solar cycle.

The field reversal process is similar in some respects to that put forth by Babcock. Toroidal fields are dragged up by vertical motions in the Rossby waves to form large-scale vertical fields, whose polarities alternate with longitude roughly like bipolar magnetic regions. Vertical fields of preferentially one polarity are carried toward the pole by the meridional motion in the wave to form an axisymmetric poloidal field. This poloidal field is then stretched out by the differential rotation into a new toroidal field of the opposite sign from the original. The poloidal field changes sign when the toroidal and bipolar region like fields are maximum, and vice versa.

For the case studied, the reversal period is too short ($\sim$ 2 years) and the poloidal fields too large ($\sim$ 40 G) for the sun. Improvements for the model are discussed.

1. Introduction

We wish to test the dynamo equations derived in Part I in a relatively simple manner. To this end, we shall replace the vertical coordinate z by just five equally spaced levels (corresponding to the middle and edges of two superposed layers of fluid), and represent horizontal variations in the variables by a small number of Fourier harmonics chosen to satisfy the boundary conditions at the sides. This technique was used successfully by Lorenz (1962, 1963) to study some aspects of thermally driven Rossby waves in the annulus.

This is a rather severe truncation of the equations, and the question naturally arises as to whether, when many more levels in the vertical and harmonics in the horizontal are added, the system will behave in basically the same way. It is possible that the smaller scale motions and magnetic fields, represented by the higher harmonics and higher vertical resolution, will drain energy away from the large scale magnetic fields faster than it can be replenished (see, e.g., Kraichnan and Nagarajan, 1967). However, since the computing time required increases roughly as the square of the number of harmonics and levels, the computing effort quickly becomes very large. For this reason, we have not yet attempted to test the convergence of the system.

To derive equations for this truncated system, it is necessary to make one further approximation. By virtue of the relation $\partial\psi^{(0)}/\partial z = \theta^{(0)}$ [Eq. (16), Part I], the boundary condition $\psi^{(0)} = 0$ at the side walls of the annulus [Eq. (28), Part I] requires that the temperature be the same on the inner and outer walls. This is very inconvenient since we wish to simulate a latitudinal temperature gradient by heating the outer half of the

* Part I has been published in *Solar Phys.* **8**, 316.

annulus and cooling the inner half. Instead of $\psi^{(0)}=0$, we can require that

$$\frac{\partial^2}{\partial y \partial t}\langle\psi^{(0)}\rangle = 0 \tag{1}$$

at the sides, where the angular brackets denote an average with respect to x around the annulus. However, with this condition, we can retain the energy integral discussed in Sec. 5F, Part I only if we drop the term $\bar{P}\mathbf{k}\cdot\nabla\times(h^{(0)}\partial\mathbf{H}_\chi^{(0)}/\partial z)$ from the vorticity Eq. (24), Part I, and $\mathbf{k}\cdot\nabla\times\partial\,(h^{(0)}\mathbf{V}_\psi^{(0)})/\partial z$ from the toroidal induction Eq. (25), Part I. Doing this is equivalent to saying that only the horizontal shears in the heliostrophic wind $\mathbf{V}_\psi^{(0)}$ are allowed to stretch poloidal fields into new toroidal fields. Leaving out stretching by the vertical shears would appear only to weaken the dynamo rather than strengthen it. In other words, if the dynamo works without this effect, and subsequent results show it does, then it will almost surely work when the vertical shear terms are included. Quantitatively, however, we should expect the dynamo to be somewhat different in the two cases. We therefore propose to ignore these terms, and use the boundary condition (1) instead of $\psi^{(0)}=0$. Clearly later models should take them into account. For the particular solutions we shall study, however, we can show that $\mathbf{k}\cdot\nabla\times\partial\,(h^{(0)}\mathbf{V}_\psi^{(0)})/\partial z$ would make a considerably smaller contribution to the induction of toroidal fields in (25), Part I than does the term $\nabla^2\mathbf{k}\cdot(\mathbf{V}_\psi^{(0)}\times\mathbf{H}_\gamma^{(0)})$.

2. Two-Layer Equations

The levels for the two-layer model are labeled 0 to 4, from bottom to top. The spacing between successive levels is denoted by $E/2$. We use ordinary centered differences to evaluate vertical derivatives. With subscripts denoting the level, the boundary conditions (12), Part I for the top and bottom approximate to

$$\psi_1^{(0)}=\psi_0^{(0)},\quad \psi_4^{(0)}=\psi_3^{(0)};\qquad \chi_1^{(0)}=\chi_0^{(0)},\quad \chi_4^{(0)}=\chi_3^{(0)};\qquad \gamma_1^{(0)}=\gamma_0^{(0)},$$
$$\gamma_4^{(0)}=\gamma_3^{(0)};\qquad h_0^{(0)}=h_4^{(0)}=0;\qquad w_0^{(0)}=w_4^{(0)}=0. \tag{2}$$

To approximate the Eqs. (22)–(25) and (27), Part I, we evaluate the variables $\chi^{(0)}$, $\psi^{(0)}$, $\gamma^{(0)}$ explicitly at levels 1 and 3, and $h^{(0)}$, $w^{(0)}$ at level 2. When we need a variable at some other level than these, we use the simple average of its values one level above and below. With this scheme, we evaluate Eqs. (22) and (25), Part I at levels 1 and 3, and Eqs. (23) and (27) at level 2. Thus, for example, using the condition $h_0^{(0)}=h_4^{(0)}=0$, Eq. (22), Part I yields

$$\nabla\cdot\mathbf{H}_{\gamma 3}^{(0)} = h_2^{(0)}/E = -\nabla\cdot\mathbf{H}_{\gamma 1}^{(0)}. \tag{3}$$

Clearly we may set $\gamma_3^{(0)}=-\gamma_1^{(0)}$, and to simplify notation we let $\gamma_3^{(0)}=\gamma$, $\gamma_1^{(0)}=-\gamma$, and $h_2^{(0)}=h$ (not to be confused with the continuous variables of Part I). Eq. (3) then gives

$$h = E\nabla^2\gamma. \tag{4}$$

Similarly, it is convenient to define $w_2^{(0)}\equiv w$ and introduce new variables ψ, τ, χ, η in the two-layer model such that $\psi_3^{(0)}=\psi+\tau$, $\psi_1^{(0)}=\psi-\tau$, $\chi_3^{(0)}=\chi+\eta$ and $\chi_1^{(0)}=\chi-\eta$.

(Again, note that ψ and χ here are distinct from the continuous variables ψ and χ of Part I.) In terms of these new variables, we can get prediction equations for $\nabla^2\psi$ and $\nabla^2\tau$ from (24), Part I, and for $\nabla^2\chi$ and $\nabla^2\eta$ from (25), Part I. We first assume $(\bar{\varrho}_1^* - \bar{\varrho}_3^*)/\bar{\varrho}_1^* \ll 1$, and define the Jacobian operator $J(a,b) \equiv \partial a/\partial x\, \partial b/\partial y - \partial a/\partial y\, \partial b/\partial x$, where a, b are any two variables. We may also set $\bar{P}=1$ without loss of generality. The boundary conditions (2) allow us to evaluate the vertical diffusion terms. The equations then are, respectively

$$\frac{\partial}{\partial t}\nabla^2\psi = -J(\psi,\nabla^2\psi) - J(\tau,\nabla^2\tau) + J(\chi,\nabla^2\chi) + J(\eta,\nabla^2\eta) + \nabla\cdot(\nabla^2\eta\nabla\gamma) + k_h\nabla^4\psi \tag{5}$$

$$\frac{\partial}{\partial t}\nabla^2\tau = -J(\tau,\nabla^2\psi) - J(\psi,\nabla^2\tau) + J(\chi,\nabla^2\eta) + J(\eta,\nabla^2\chi) + \nabla\cdot(\nabla^2\chi\nabla\gamma) - w/E + k_h\nabla^4\tau - k_v\nabla^2\tau \tag{6}$$

$$\frac{\partial}{\partial t}\nabla^2\chi = -\nabla^2 J(\psi,\chi) - \nabla^2 J(\tau,\eta) + \nabla^2(\nabla\gamma\cdot\nabla\tau) + b_h\nabla^4\chi \tag{7}$$

$$\frac{\partial}{\partial t}\nabla^2\eta = -\nabla^2 J(\psi,\eta) - \nabla^2 J(\tau,\chi) + \nabla^2(\nabla\gamma\cdot\nabla\psi) + b_h\nabla^4\eta - b_v\nabla^2\eta. \tag{8}$$

In the above equations $k_h = 1/R_L$, $k_v = 4/R_D E^2$, $b_h = 1/G_L$, $b_v = 4/G_D E^2$ (the subscripts h and v refer to horizontal and vertical diffusion, respectively).

From (27), Part I, using (4), we can find a prediction equation for $\nabla^2\gamma$, given by

$$\frac{\partial}{\partial t}\nabla^2\gamma = -J(\psi,\nabla^2\gamma) + RoJ(\chi,w)/E + b_h\nabla^4\gamma - \tfrac{1}{2}b_v\nabla^2\gamma. \tag{9}$$

Finally, from the thermodynamic Eq. (23), Part I, we can obtain, (defining $\varepsilon' = E/2\varepsilon$, $q_h = 1/G_L$, $q_v = 2/C_D E^2$)

$$\frac{\partial\tau}{\partial t} = -J(\psi,\tau) - \varepsilon' w + q_h\nabla^2(\tau - \hat{\tau}) - q_v(\tau - \hat{\tau}). \tag{10}$$

In (10) we have represented the forcing function Q in terms of a prescribed 'temperature' $\hat{\tau}$ toward which the convection is always trying to push the 'temperature' field. $\hat{\tau}$ will be chosen as a simple function of y, representing a warm equatorward side of the annulus and a cold poleward side (the *net* heating over the whole annulus will be zero). The vertical temperature structure, also determined primarily by the convection, is contained in ε', which we assume constant.

3. Truncated Harmonic Equations

The six Eqs. (5)–(10) now comprise the prediction equations for the two-layer dynamo, predicting the six two-layer variables ψ, τ, χ, η, w, γ. The boundary conditions at the top and bottom have been incorporated directly into these equations. The

boundary conditions at the sides for the two-layer variables are, from (11), Part I, (28), Part I (for $\chi^{(0)}$ only), (1) and (4),

$$\frac{\partial\psi}{\partial x}, \frac{\partial\tau}{\partial x}, \frac{\partial^2\langle\psi\rangle}{\partial y\,\partial t}, \frac{\partial^2\langle\tau\rangle}{\partial y\,\partial t}, \chi, \eta, \frac{\partial^2\chi}{\partial y^2}, \frac{\partial^2\eta}{\partial y^2}, \frac{\partial\gamma}{\partial y}, \frac{\partial}{\partial y}\nabla^2\gamma = 0. \tag{11}$$

The next step is to expand each variable in a set of normalized orthogonal Fourier harmonics each of which satisfies the appropriate boundary conditions. We note that w, which has no boundary conditions at the sides, is completely determined by (6) and (10) if there are no magnetic fields and ψ and τ are known. It is therefore natural to expand w in the same harmonics we use for ψ and τ.

Let us take the side walls of the annulus at $y=0, +\pi$, and also let x vary from 0 to 2π. Since we are describing the annulus in Cartesian geometry, we have, in effect, replaced it by an infinite or periodic channel. The dimensionless length L really need not be commensurate with the annulus circumference, but can be compared to a longitudinal 'wavelength' of bipolar magnetic regions on the sun. With $0\leqslant y\leqslant\pi$, $0\leqslant x\leqslant 2\pi$, we define the following normalized harmonic functions:

$$\begin{aligned} f_{mo} &= 2^{-1/2}\cos my; \quad f_{mn} = 2^{-1}\cos my\cos nx; \quad f'_{mn} = 2^{-1}\cos my\sin nx \\ g_{mo} &= 2^{-1/2}\sin my; \quad g_{mn} = 2^{-1}\sin my\cos nx; \quad g'_{mn} = 2^{-1}\sin my\sin nx. \end{aligned} \tag{12}$$

Then the appropriate expansions for ψ, τ, w are (using upper case symbols for the amplitude coefficients, which are functions of time only)

$$\psi, \tau, w = \sum_{m=1}^{\infty}(\Psi_{mo}, T_{mo}, W_{mo})\,f_{mo} + \sum_{m,n=1}^{\infty}(\Psi_{mn}, T_{mn}, W_{mn})\,g_{mn} + \sum_{m,n=1}^{\infty}(\Psi'_{mn}, T'_{mn}, W'_{mn})\,g'_{mn}. \tag{13}$$

Similarly, for χ, η, we have

$$\chi, \eta = \sum_{m=1}^{\infty}(X_{mo}, H_{mo})\,g_{mo} + \sum_{m,n=1}^{\infty}(X_{mn}, H_{mn})\,g_{mn} + \sum_{m,n=1}^{\infty}(X'_{mn}, H'_{mn})\,g'_{mn}. \tag{14}$$

Finally, for γ, we have

$$\gamma = \sum_{m=1}^{\infty}\Gamma_{mo}f_{mo} + \sum_{m,n=1}^{\infty}\Gamma_{mn}f_{mn} + \sum_{m,n=1}^{\infty}\Gamma'_{mn}f'_{mn}. \tag{15}$$

We can represent the thermal forcing $\hat{\tau}$ by a series completely analogous to (13).

In general, then, by substituting these expressions into Eqs. (5)–(10), then multiplying by each harmonic in succession and integrating over the domain $0\leqslant y\leqslant\pi$, $0\leqslant x\leqslant 2\pi$, we can obtain an infinite set of *ordinary* nonlinear differential equations in time for the amplitude coefficients of each of the variables. The nonlinear terms represent interactions between different harmonics. In the absence of thermal forcing

and dissipation, we can find an energy integral analogous to that discussed in Sec. 5F, Part I.

Obviously, to obtain a closed system, we must truncate the harmonic series. Lorenz (1963) was able to obtain useful results for the Rossby wave problem without magnetic fields with a system in which he retained only harmonics for $m=1, 2$ together with a single nonzero value of $n=2$, as well as $n=0$. The nonlinear interaction terms in the equations, then, involve interactions only among the harmonics of this set. Interactions with higher harmonics are discarded. The truncated system still conserves energy when forcing and dissipation are suppressed.

We propose to truncate our system in exactly the same way. The results of Lorenz (1963) then, will serve as a useful guide for what to expect from our system without magnetic fields, although his choice of boundary conditions at the bottom of the annulus is somewhat different.

With the truncation we have chosen, each of the six variables is represented by six harmonics: four with longitude (x) and latitude (y) dependence, and two with only latitude dependence. Thus from (5)–(10) we would obtain a system of thirty-six ordinary differential equations. It is convenient to replace the double subscript and prime notation for the amplitude coefficients in this truncated system by single letters, following Lorenz (1963). Thus if Z is an amplitude coefficient for any of the variables $\psi, \tau, w, \chi, \eta, \gamma$, we let $Z_{10}=Z_A$, $Z_{11}=Z_K$, $Z'_{11}=Z_L$, $Z_{20}=Z_C$, $Z_{21}=Z_M$, $Z'_{21}=Z_N$. The A, C modes for each variable, then, are the symmetric modes, and the K, L, M, N modes are the longitudinally varying or 'Rossby wave' modes.

These modes can be broken down further into two groups of eighteen such that if no harmonics from one group are excited initially, they will remain unexcited. To thermally force the system we chose $\hat{\tau}=\hat{T}_A 2^{-1/2}\cos y$ (as did Lorenz, 1963), which represents a temperature monotonically decreasing from the equator (outer edge of the annulus) toward the pole. The eighteen modes that group with $\hat{T}_A$ are

$$\begin{aligned} &T_A,\ T_L,\ T_M,\ \Psi_K,\ \Psi_C,\ \Psi_N \\ &W_A,\ W_L,\ W_M,\ X_A,\ X_K,\ X_N \\ &H_L,\ H_C,\ H_M,\ \Gamma_A,\ \Gamma_K,\ \Gamma_N. \end{aligned} \tag{16}$$

The study of just these modes will give sufficient indication of the dynamo properties of the system. Within this set, we can think of T_A, Ψ_C as representing the axisymmetric 'differential rotation', and W_A as the axisymmetric meridian circulation. The modes $T_L, T_M, \Psi_K, \Psi_N, W_L, W_M$, then represent the 'Rossby waves', in this case with a single longitudinal wavelength. Similarly, X_A and H_C comprise the axisymmetric toroidal field, while Γ_A is the symmetric poloidal field. The modes $X_K, X_N, H_L, H_M, \Gamma_K, \Gamma_N$ give the magnetic structure of the Rossby wave, which we might identify with the bipolar magnetic regions of the sun. $\Gamma_A, \Gamma_K, \Gamma_N$, being related to the vertical field h [by (15) and (4)], can be compared to the observed large-scale solar fields.

Defining $r=\sqrt{2}$, $s=4r/15\pi$, setting $E=1$, $\varepsilon'=0.1$, and letting dots denote time differentiation, we may now write down the eighteen differential equations for the amplitudes (16).

$$\dot{\Psi}_K = -16sT_LT_A - \frac{128s}{5}\Psi_N\Psi_C - \frac{7r}{5}X_AX_N + \frac{2r}{5}H_CH_L - \frac{6r}{5}H_C\Gamma_K + \frac{4r}{5}H_M\Gamma_A - 5k_h\Psi_K \quad (17)$$

$$\dot{\Psi}_C = 24s(\Psi_K\Psi_N - T_MT_L - X_KX_N + H_MH_L) - 16sH_C\Gamma_A - 40sH_L\Gamma_N - 32sH_M\Gamma_K - 4k_h\Psi_C \quad (18)$$

$$\dot{\Psi}_N = 14sT_AT_M + 4s\Psi_K\Psi_C + \frac{r}{2}X_AX_K - \frac{5r}{8}H_L\Gamma_A - 8k_h\Psi_N \quad (19)$$

$$\dot{T}_A = W_A - 10sX_A\Gamma_A - 50sX_K\Gamma_K - 128sX_N\Gamma_N - (k_h + k_v)T_A \quad (20)$$

$$\dot{T}_L = \frac{1}{5}W_L + 16s\Psi_KT_A + \frac{128s}{5}T_M\Psi_C + \frac{7r}{5}X_AH_M - \frac{2r}{5}H_CX_K + \frac{4r}{5}X_N\Gamma_A + \frac{3r}{5}X_A\Gamma_N - (5k_h + k_v)T_L \quad (21)$$

$$\dot{T}_M = \frac{1}{8}W_M - 14s\Psi_NT_A - 4sT_L\Psi_C - \frac{r}{2}X_AH_L - \frac{5r}{8}X_K\Gamma_A - \frac{3r}{8}X_A\Gamma_K - (8k_h + k_v)T_M \quad (22)$$

$$\dot{T}_A = 20s\Psi_KT_L - 16s\Psi_NT_M - \varepsilon' W_A - (q_v + q_h)(T_A - \hat{T}_A) \quad (23)$$

$$\dot{T}_L = -20s\Psi_KT_A + 32s\Psi_CT_M - \varepsilon' W_L - (q_v + 5q_h)T_L \quad (24)$$

$$\dot{T}_M = 16s\Psi_NT_A - 32s\Psi_CT_L - \varepsilon' W_M - (q_v + 8q_h)T_M \quad (25)$$

$$\dot{X}_A = r(X_K\Psi_N - X_N\Psi_K + H_MT_L - H_LT_M) + 10sT_A\Gamma_A + 3r(T_M\Gamma_K - T_L\Gamma_N) - b_hX_A \quad (26)$$

$$\dot{X}_K = -rX_A\Psi_N + 2rH_CT_L - 20sH_LT_A - 32sX_N\Psi_C + 10sT_A\Gamma_K + rT_M\Gamma_A - 5b_hX_K \quad (27)$$

$$\dot{X}_N = rX_A\Psi_K + 16sH_MT_A + 32sX_K\Psi_C + 16sT_A\Gamma_N - \frac{r}{2}T_L\Gamma_A - 8b_hX_N \quad (28)$$

$$\dot{H}_L = rX_AT_M - 2rH_C\Psi_K + 20sX_KT_A + 32s(H_M\Psi_C + \Psi_C\Gamma_N) + r\Psi_N\Gamma_A - (5b_h + b_v)H_L \quad (29)$$

$$\dot{H}_C = 2r(H_L\Psi_K - X_KT_L) + 16s\Psi_C\Gamma_A + \frac{3r}{2}\Psi_K\Gamma_K - (4b_h + b_v)H_C \quad (30)$$

$$\dot{H}_M = -rX_AT_L - 16sX_NT_A - 32sH_L\Psi_C + 16s\Psi_C\Gamma_K - \frac{r}{2}\Psi_K\Gamma_A - (8b_h + b_v)H_M \quad (31)$$

$$\dot{\Gamma}_A = -5r\Psi_N\Gamma_K - 8r\Psi_K\Gamma_N + 4sRo(5W_LX_K - 4W_MX_N) - \left(b_h + \frac{b_v}{2}\right)\Gamma_A \quad (32)$$

$$\dot{\Gamma}_K = -\frac{64s}{5}\Psi_C\Gamma_N + \frac{r}{5}\Psi_N\Gamma_A + Ro\left(\frac{r}{5}X_N W_A + 2sX_A W_L\right) - \left(5b_h + \frac{b_v}{2}\right)\Gamma_K \tag{33}$$

$$\dot{\Gamma}_N = 5s\Psi_C\Gamma_K + \frac{r}{8}\Psi_K\Gamma_A + \frac{r}{8}RoX_K W_A - \left(8b_h + \frac{b_v}{2}\right)\Gamma_N . \tag{34}$$

4. Numerical Integration Procedure

For all cases, we fix the thermal forcing $\hat{T}_A = 0.5$, and let $Ro = 0.1$. Furthermore, to reduce the number of parameters, we let $q_v = 2q_h \equiv q$, $k_v = 4k_h \equiv k$, $b_v = 4b_h \equiv b$. This is equivalent to letting $D = L$, so that horizontal and vertical diffusion are roughly of equal magnitude (actually horizontal diffusion is larger for the high horizontal wave numbers, vertical diffusion bigger for the low wave numbers). Finally, we let $q = k$. This is equivalent to fixing the effective Prandtl number $\nu/\kappa = 0.5$, which does not seem unreasonable for solar turbulence. In summary, then, q is proportional to the effective thermal and mechanical diffusion, while b is proportional to the magnetic diffusion or resistivity.

Since we are taking $L = 1.5 \times 10^5$ km, assuming $D = L$ is inconsistent with our original statement in Part I, Sec. 3 that the depth of the annulus is not much larger than a scale height. Since we have also taken $(\bar{\varrho}_3^* - \bar{\varrho}_1^*)/\bar{\varrho}^* \ll 1$ for the two-layer model, we are in effect dealing now with a stratified *liquid*, with mean density that of the convection zone, contained in an annulus with roughly the depth of the convection zone and of width perhaps 40° latitude.

To integrate Eqs. (17)–(34) in time we replace the time derivatives by a two-step finite difference form, the so-called Adams-Bashforth scheme. This scheme has been tested and found satisfactory for problems of our type by Lilly (1965). With this form, if

$$\dot{Y} = f(t) \tag{35}$$

is any of our differential equations, the value of Y at time t_{i+1} is given in terms of quantities computed for the previous two time steps t_i, t_{i-1} according to the formula

$$Y(t_{i+1}) = Y(t_i) + \left[\tfrac{3}{2}f(t_i) - \tfrac{1}{2}f(t_{i-1})\right]\Delta t . \tag{36}$$

where Δt is the time increment between steps. Eq. (36) works for all but the first time step, for which we use an ordinary forward difference, given by

$$Y(\Delta t) = Y(0) + f(0)\,\Delta t \tag{37}$$

The value of Δt used is chosen when successive integrations with decreasing Δt, for fixed values of all other parameters, show little difference in behavior (amplitudes, periods, etc.) after several thousand time steps. In all cases, $\Delta t = 0.25$ was found to be satisfactory for our purposes.

To actually integrate (17)–(34), using (36) and (37), we proceed as follows. First, we specify nonzero but small initial values for T_A, Ψ_K, Ψ_N (following Lorenz, 1963). The magnetic field is initially kept equal to zero. Then, eliminating T_A, T_L, T_M from

(20)–(25), we may find consistent initial values for W_A, W_L, W_M. Then from (17)–(23), using (37), we find new values for $\Psi_{K,C,N}$; $T_{A,L,M}$ at $t=\Delta t$, and then use (36) to determine $\Psi_{K,C,N}$; $T_{A,L,M}$ at $t=2\Delta t$. Thereafter the process is repeated for each Δt increment. Doing this, we allow the solution without magnetic fields to develop until it has reached its final form (we discuss the various types of solutions without magnetic fields in the next section). At this point, usually after at least 10^3 time steps, we insert a small value for one of the magnetic field components, say X_A, so small that at first the Maxwell stresses have no significant effect on the motion. Eq. (26)–(34), together with (37), then provide values for all the magnetic amplitudes at later times. The magnetic fields then either grow or decay, depending upon how large a resistivity (proportional to b) we choose. The integration is terminated when it is clear that further iterations will not yield any new information.

5. Solutions Without Magnetic Fields

As stated earlier, our model without magnetic fields, represented by Eqs. (17)–(25), is very similar to that studied by Lorenz (1963). We can therefore classify the solutions in the same manner as he did. Roughly speaking, as we reduce q (corresponding to reduced effective thermal conductivity and viscosity) the solutions become more turbulent. In the neighborhood of $q=0.24$, we get steady Rossby-wave solutions in which all nine modes for the motion approach nonzero constant values after sufficient time. We will concentrate on the dynamo properties of this type of solution. For somewhat larger values of q, we find steady Rossby-wave solutions in which only five of the nine modes (Ψ_K, T_A, T_L, W_A, W_L) are present. For still higher q, we find only the axisymmetric modes T_A, W_A are produced, corresponding to a meridian circulation and zonal flow or differential rotation.

For q somewhat smaller than 0.24, we find that all nine modes are present, but rather than being steady they oscillate about mean values close to the solution for $q=0.24$. As q is decreased still further, the amplitude of the oscillation becomes larger. A typical oscillation period is 20 dimensionless time units. These are called vacillating solutions. All of the above solutions correspond qualitatively to observed motions in rotating annulus laboratory experiments.

Because the boundary conditions at the top and the bottom of the annulus are the same, our Rossby waves are standing waves relative to the rotating coordinate system. If we had required no slip at the bottom, which is approximately what Lorenz did, we would have found the waves moved around the annulus slightly faster than the basic rotation. We have also looked at the dynamo properties of these waves, and found them to be quite similar to what we shall report below for the standing Rossby waves.

6. Analysis of a Solution with Reversing Magnetic Fields

A. THE INDUCTION PROCESS

We shall analyze here in detail the dynamo action of the steady Rossby-wave solution

for the thermal and viscous diffusion parameter $q=0.24$. The results for this case are typical of the dynamo behavior of the Rossby wave motions in general. To find the Rossby wave solution, we initially set $T_A=10^{-2}$, $\Psi_K=5\times10^{-3}$, $\Psi_N=-5\times10^{-3}$, with Ψ_C, T_L, T_M and all the magnetic amplitudes equal to zero. After two thousand iterations with $\Delta t=0.25$, a steady state is well established, for which

$$\begin{aligned} \Psi_K &= 1.479\times10^{-1}; & \Psi_C &= -7.702\times10^{-2}; & \Psi_N &= -3.527\times10^{-2} \\ T_A &= 3.953\times10^{-1}; & T_L &= -6.945\times10^{-2}; & T_M &= -1.725\times10^{-2} \\ W_A &= 1.186\times10^{-1}; & W_L &= -7.695\times10^{-1}; & W_M &= -2.663\times10^{-1}. \end{aligned}$$

At this point, we set $X_A=5\times10^{-3}$, and proceed with the integration for three thousand more iterations. One run of this length typically took about two minutes on a CDC 6400 computer. The results are presented in Figures 1–3. All the magnetic field amplitudes oscillate periodically about zero, with a period of around 160 time increments. The peak amplitudes of X_A (denoted by + and −) are plotted in Figure 1, for four different values of b, the magnetic diffusion parameter. We note that the period of field reversal is rather insensitive to b, but whether the peaks grow or decay is strongly dependent on it. The 'dynamo threshold', for b values smaller than which the successive peaks amplify, is for the present case $b\approx0.04$. Since for $E=1$, $b=4/G_L$, $b=0.04$ corresponds to effective magnetic Reynolds numbers $G_D=G_L=100$.

For $b=0.03$, the peaks level off after 3600 increments. Up to this point, the inducing motions are virtually unchanged from their steady values found from the first 2000 interations. Beyond this time the fields are large enough so that the Maxwell stresses, reacting upon the motion, modify it in such a way as to reduce further induction to

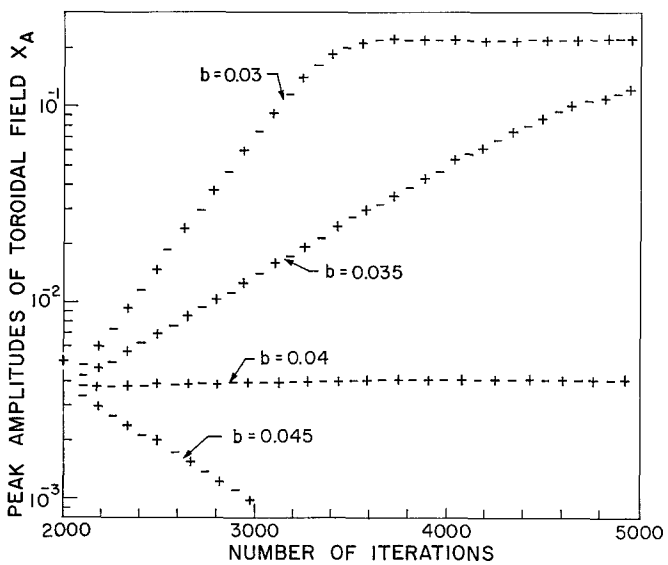

Fig. 1. Peak amplitudes (+ and −) of the principal toroidal field amplitude X_A as a function of the number of iterations. Solution is for mechanical and thermal diffusion parameter $q=0.24$; b is the magnetic diffusion parameter.

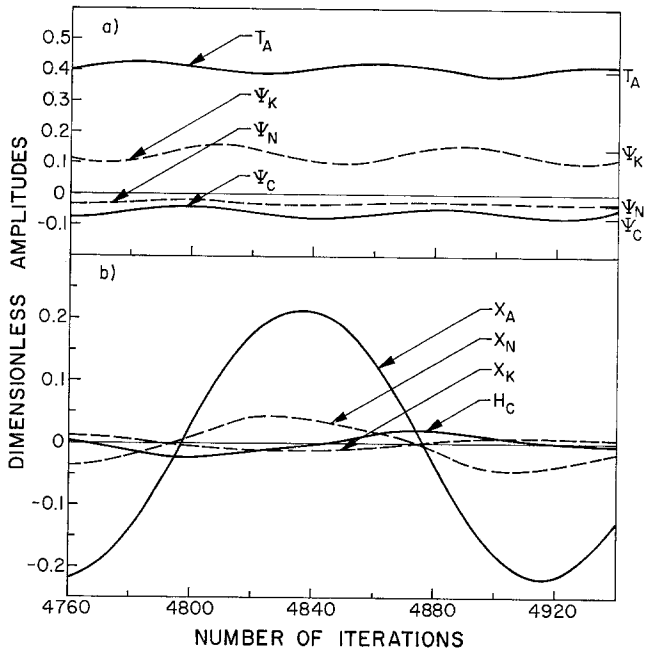

Fig. 2. (a) Amplitudes of selected harmonics for the Rossby wave (Ψ_K, Ψ_N; dashed lines) and differential rotation (T_A, Ψ_C; solid lines) for one complete cycle with $b = 0.03$. Hatch marks on the right edge indicate values of these amplitudes without magnetic fields. (b) Amplitudes of the toroidal field for the same cycle.

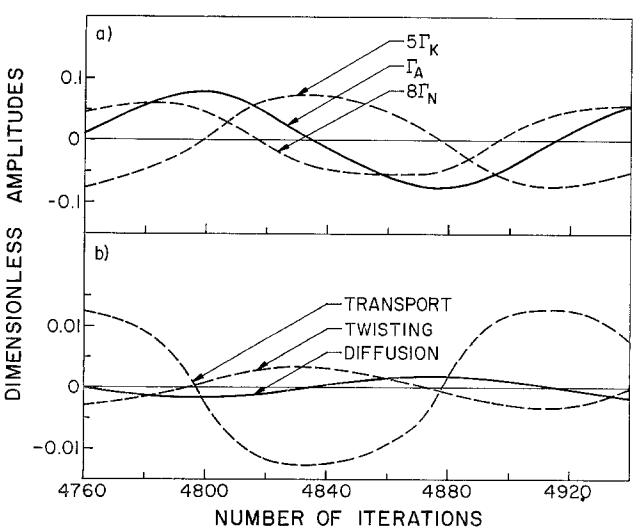

Fig. 3. (a) Amplitudes of the vertical magnetic fields for the same cycle as in Figure 2. (b) Analysis of the processes determining the axisymmetric vertical field Γ_A for the same cycle.

the point that, on the average over a cycle, induction of fields is balanced by diffusion. The field reversal period is changed very little by this effect. The peak energy in the magnetic field once the balance is achieved is about 25% of the energy in the horizontal motion. Note that if the reaction of the induced fields on the flow had not been included, successive peaks in the field amplitudes would have continued to grow without limit.

We have also looked at the dynamo behavior for $b=0.025$, (not plotted) and have found that the peaks grow still faster, but once the Maxwell stresses are large enough to alter the motion, successive peaks do not settle down to steady values, but rather fluctuate rather irregularly with a variation of a factor of two or so. The average value of the peaks is, however, close to that for $b=0.03$.

The details of the field-reversal process and reaction of the fields on the flow are illustrated in Figures 2 and 3 for one cycle with $b=0.03$. In Figure 2a, we have plotted representative amplitudes for the motion. We note that the reversing fields induce an oscillation in the motion with period one-half that of the field oscillations. These oscillations, however, represent only small modulation of the motion without magnetic fields, indicated by the labelled marks on the right-hand edge of the figure. The total kinetic energy of the motion changes by no more than 10% over an oscillation. That the period of oscillation in the motion is half that of the magnetic field is reasonable, since the Maxwell stress is invariant to a change in sign of all field components. The stress acts in the same way on the motion at corresponding points in successive half cycles of the field.

Figure 2b shows the cyclic variations in the toroidal field amplitudes X_A, X_K, X_N, H_{CT} (H_L, H_M, not plotted, have about the same amplitudes and variations as X_K, X_N), while Figure 3a gives variations in the poloidal field. The poloidal harmonics are weighted so that each curve is proportional to the *vertical* magnetic field for that harmonic. We do this for easier comparison with the observed radial fields on the sun.

We note that the bulk of the toroidal fields (X_A, X_K, X_N, H_L, H_M) are strongest when the *symmetric* poloidal field Γ_A is changing sign. On the other hand, the *asymmetric* poloidal fields Γ_K and Γ_N are largest at about the same time the toroidal fields are largest.

A careful examination of the various nonlinear interactions in the induction Eqs. (26)–(34) reveals the dominant feedbacks which comprise the reversal process. From X_A, the vertical motion W_L in the Rossby wave produces vertical fields in the form of Γ_K [through the term $2sRoX_AW_L$ in Eq. (33)]. Some of this vertical field is transported across the channel by the meridional motion of the Rossby wave associated with Ψ_N to increase the axisymmetric poloidal field Γ_A (represented by the terms $(r/5)\Psi_N\Gamma_A$ in (33) and $-5r\,\Psi_N\Gamma_K$ in (32)). In addition, some of Γ_K is transformed into Γ_N by Ψ_C, whence into Γ_A by the horizontal transport due to Ψ_K of the Rossby wave (through the terms $-(64s/5)\Psi_C\Gamma_N$ in (33), $5s\Psi_C\Gamma_K$ and $(r/8)\Psi_K\Gamma_A$ in (34), and $-8r\Psi_K\Gamma_N$ in (32)). Finally, the induced poloidal field Γ_A, by interacting with T_A, which represents the bulk of the differential rotation, is stretched put into a new toroidal field X_A *of the opposite sign from the original.* [This is accomplished by the term $10sT_A\Gamma_A$ in (26)]. Then the induction of new Γ_K, Γ_N repeats but with signs reversed. The other non-linear

interactions also contribute to the reversal process, of course, but in lesser amounts.

For dynamo solutions, then, the terms representing the twisting of toroidal fields into the vertical by vertical motions in the Rossby waves, which are multiplied by Ro in Eqs. (22)–(34), are as large as all other terms in these equations, despite the fact that they are formally of higher order in Rossby number.

The processes determining the size of the symmetric poloidal field are evaluated in Figure 3b. Taking terms from Eq. (33), we define

$$-5r\Psi_N\Gamma_K - 8r\Psi_K\Gamma_N \equiv \text{transport}$$
$$4sRo(5W_LX_K - 4W_MX_N) \equiv \text{twisting}$$
$$-(b_h + bv/2)\,\Gamma_A \equiv \text{diffusion}.$$

Comparison of the transport curve in Figure 3b with the variations seen in Figure 3a clearly shows that the horizontal transport of vertical fields by the Rossby waves produces Γ_A. When this transport is positive, Γ_A is becoming increasingly positive; when it is negative, Γ_A is becoming more negative. The transport process is opposed by the vertical motions W_L, W_M of the Rossby wave twisting toroidal fields X_K, X_N into the vertical to partially cancel the flux in Γ_A. Finally, diffusion, of course, is always trying to reduce the magnitude of Γ_A.

Plots similar to Figure 3b for the other induction equations can be constructed to reveal the rest of the induction process described above.

B. OTHER DYNAMO SOLUTIONS

We have also looked at the dynamo action of flows for q somewhat larger and somewhat smaller than 0.24. For larger q, when only the five harmonics T_A, T_L, Ψ_K, W_A, W_L are excited, we found that when a small magnetic field is added, all nine magnetic harmonics are excited. Then the reaction upon the motion excites the remaining amplitudes Ψ_C, Ψ_N, T_M, W_M of the motion. Thereafter the solution behaves in much the same way as the one discussed in detail above.

For q smaller than 0.24, in the region of vacillating motions, we find that, in general, when the induced fields are large enough to influence the motion, the original vacillation period is suppressed and replaced by the oscillation at one-half the period for field reversals. The periods for all solutions looked at vary by no more than 20%.

As mentioned in Sec. 5, we have also looked at the dynamo behavior of Rossby-type motions subject to different boundary conditions. In particular, if we allow no slip at the bottom of the channel, the boundary condition on $\psi^{(0)}$, used to evaluate the vertical diffusion of vorticity $\partial^2/\partial z^2\,\nabla^2\psi^{(0)}$ for the two-layer model, is that $\psi_0^{(0)}=0$. With this asymmetry in the boundary conditions (since $\psi_3^{(0)}=\psi_4^{(0)}$), it can be shown that all thirty-six amplitudes are linked, instead of being broken into two non-interacting groups of eighteen. Also the Rossby waves are not stationary, but instead propagate around the channel. Nevertheless, we have found that reversing magnetic fields with roughly the same period are produced by these motions too.

C. EFFECT OF NEGLECTED TERMS

We need to assess as far as practical the effects by the various terms we have neglected

on the field reversal process we have presented above. First, since only Eq. (9) for the vertical field $h=E\nabla^2\gamma$ contains a term formally of higher order in Rossby number [the term $RoJ(\chi,w)/E$], we should examine all the other terms of this order which would have been present in this equation had we not chosen to ignore them for reasons discussed in Part I, Sec. 5E. Before approximating to the two-layer model, these terms are, from the right hand side of Eq. (8), Part I (dropping the Ro^2 factor)

$$(\mathbf{H}_\gamma^{(0)}\cdot\nabla)\,w^{(0)}-(\mathbf{V}_\sigma^{(0)}\cdot\nabla)\,h^{(0)}+w^{(0)}\nabla\cdot\mathbf{H}_\gamma^{(0)}-h^{(0)}\nabla\cdot\mathbf{V}_\sigma^{(0)}. \tag{35}$$

For the two-layer system, these terms, evaluated at level 2, at which Eq. (9) applies, become

$$\frac{(\mathbf{H}_{\gamma1}^{(0)}+\mathbf{H}_{\gamma3}^{(0)})}{2}\cdot\nabla w_2^{(0)}-\frac{(\mathbf{V}_{\sigma1}^{(0)}+\mathbf{V}_{\sigma3}^{(0)})}{2}\cdot\nabla h_2^{(0)}+w_2^{(0)}\nabla\cdot\frac{(\mathbf{H}_{\gamma1}^{(0)}+\mathbf{H}_{\gamma3}^{(0)})}{2}$$
$$-h_2^{(0)}\nabla\cdot\frac{(\mathbf{V}_{\sigma1}^{(0)}+\mathbf{V}_{\sigma3}^{(0)})}{2}. \tag{36}$$

We show now that all these terms actually vanish. We have already shown in Sec. 2 from Eq. (3) that for the two layer model we may set $\gamma_3^{(0)}=-\gamma_1^{(0)}$, so that $\mathbf{H}_{\gamma3}^{(0)}=-\mathbf{H}_{\gamma1}^{(0)}$ and therefore $\mathbf{H}_{\gamma1}^{(0)}+\mathbf{H}_{\gamma3}^{(0)}=0$. This means the first and third terms in (36) vanish.

Since we are assuming also that $(\bar\varrho_1^*-\bar\varrho_3^*)/\bar\varrho_1^*\ll1$, we can show by approximating Eq. (20), Part I for the two layer model that

$$\nabla\cdot\mathbf{V}_{\sigma3}^{(0)}=w_2^{(0)}/E=-\nabla\cdot\mathbf{V}_{\sigma1}^{(0)} \tag{37}$$

Eq. (35) is completely analogous to Eq. (3) for the poloidal field, so that we may set $\sigma_1^{(0)}=-\sigma_3^{(0)}$ and consequently $\mathbf{V}_{\sigma1}^{(0)}+\mathbf{V}_{\sigma3}^{(0)}=0$. Therefore the second and fourth terms in (36) drop out. Of course, when we go to more sophisticated models, with more levels in the vertical, the corresponding form for (35) may no longer vanish.

For reasons discussed in Sec. 1, we also ignored in the induction equation for toroidal field the term $\mathbf{k}\cdot\nabla\times\partial\,(h^{(0)}\mathbf{V}_\psi^{(0)})/\partial z$. For the two-layer model this term approximates to $\mathbf{k}\cdot\nabla\times[h_2^{(0)}(\mathbf{V}_{\psi1}^{(0)}+\mathbf{V}_{\psi3}^{(0)})]/2E$ at level 1, and the negative of this at level 3. These will together add a term $-(\nabla\cdot\nabla^2\gamma\nabla\psi)$ to the right hand side of (8). Since (8) is the prediction equation for $\nabla^2\eta$ from which we obtain (29), (30), (31) for H_L, H_C, H_M, we expect that these harmonics will be somewhat different, but certainly not larger by an order of magnitude. On the other hand, the forms of (26)–(28) for the amplitudes X_A, X_K, X_N are *unchanged*, as are (32)–(34) for the poloidal fields Γ_A, Γ_K, Γ_N. We have shown that the dominant toroidal field in the reversal process is X_A. Its magnitude is determined in (26) primarily by the interaction $10sY_A\Gamma_A$ of the differential rotation and poloidal field. The interactions involving H_L and H_M are smaller typically by a factor of ten, so that the changes in H_L, H_M caused by the additional terms in (29), (30) and (31) should have little effect. Since in addition, Eqs. (32)–(34) for the poloidal fields do not even contain H, the principal reversal process should not be altered significantly.

Finally, since terms formally of higher order in Rossby number in the *poloidal* field induction Eqs. (32)–(34) are in fact as large as the other terms in these equations, it is legitimate to ask whether this would be true of higher-order terms we have omitted from the toroidal field induction equations. However, we find for our solutions that these terms are in fact as small as they should be according to the Rossby number expansion.

In summary, then, within the context of a two-layer, truncated harmonic model, we feel we have captured the principal processes responsible for the dynamo maintenance and reversal of the magnetic fields.

7. Comparison with Solar Observations

Our dynamo model is sufficiently idealized that we really can make only qualitative and order-of-magnitude comparisons to the solar cycle. First of all, the period of magnetic field reversal in our solution is about 160 iterations for $\Delta t = 0.25$. Given the time scale $L/U = 1.5 \times 10^6$ sec, this is in real time 6×10^7 sec, or two years, compared to about 20 years for the actual solar cycle. Peak energies in the toroidal field for our model are about 25% of the kinetic energy of flow. This means a peak toroidal field strength $M_T = \pi^{1/2} \varrho^{1/2} U$, so that for $\varrho \approx 10^{-4}$ g cm^{-3}, $U = 100$ m sec^{-1}, $M_T = 180$ G. The peak energy in the symmetric vertical field Γ_A, corresponding to the sun's polar field, and in the 'bipolar magnetic region' fields Γ_K, Γ_M are each about 6% of the total toroidal field energy. Therefore these peak field strengths are about 40 G, about one order of magnitude larger than observed on the sun. Obviously, since our model is incompressible and highly truncated, our estimates are crude. Also, choosing a δ smaller than one would reduce the vertical fields proportionately.

We can summarize the process of field reversal in our model in three steps. 1. Vertical motions in the Rossby waves drag up toroidal field lines to make large-scale vertical fields. 2. These are in turn transported in latitude to form the axisymmetric poloidal field. 3. This poloidal field is then stretched out by the differential rotation into a new toroidal field of the opposite sign. This sequence fits well with, for example, Babcock's (1961) conception of the reversal process. Babcock invoked magnetic buoyancy to produce vertical flux instead of large-scale vertical motions, but he did postulate meridional currents to transport flux poleward, as well as the differential rotation stretching the poloidal into a new toroidal field. Bumba and Howard (1965) have observed the poleward migration of vertical flux, but could not say whether large-scale mass motions were producing it.

Other properties of our model also have their counterparts in the observations. For example, the poloidal field Γ_A in our model is a maximum when Γ_K, Γ_N and the toroidal field are changing signs. This corresponds roughly to solar activity minimum. When Γ_A changes sign, the rest of the fields are maximum, corresponding to activity maximum. Also, through the dynamo cycle the horizontal flow varies only a moderate amount (10%). So far as is known, the sun's differential rotation does not undergo large variations with the solar cycle either.

In general, our dynamo is much more 'coherent' than is the sun. That is, the field-reversal process is much smoother as well as faster. This is presumably because the motion and fields have so few degrees of freedom. We would expect on the sun (and in a model with many more degrees of freedom) that individual Rossby wave disturbances would grow and die (corresponding perhaps to the birth and decay of active regions), each successive disturbance making its contribution to the reversal process. It would seem from this that there would be more local cancellation of magnetic flux and that probably the cycle would proceed more slowly and with somewhat smaller amplitudes.

Within our model, it is possible to achieve longer periods simply by reducing the Rossby number. Decreasing it by a factor of three would give reversal periods of ≈ 20 years. However, this small a Rossby number would correspond to a solar differential rotation smaller than is observed.

For the dynamo solution most thoroughly studied above (with $q=0.24$, $b=0.03$ and $\delta=1$) the turbulent viscosity is $\nu \approx 10^{13}$ cm^2 sec^{-1}, while the thermal diffusion coefficient $\kappa \approx 2\times 10^{13}$ cm^2 sec^{-1}. The former is in line with values given in Cocke (1967). The effective resistivity $\lambda \approx 1.5\times 10^{12}$ cm^2 sec^{-1}, which is two orders of magnitude smaller than used by Leighton (1964) for diffusion of bipolar magnetic region fields toward the pole. However, in our model, Leighton's diffusion process that forms the polar field is replaced by the transport of vertical fields by the mass motions in the Rossby waves.

Finally, we can make an estimate of the latitudinal temperature gradient needed for the dynamo. Again, since our model does not take account of compressibility, this is crude. As stated in Gilman (1968), the temperature difference ΔT between equator and pole is given by the thermal wind relation so that

$$\Delta T \approx (m\Omega/R)(\pi a/2)(U/N)$$

where R is the universal gas constant, m the molecular weight, a the sun's radius, and N the number of pressure scale heights the fluid layer is deep. For $m=\frac{1}{2}$ (ionized hydrogen), $a=7\times 10^{10}$ cm, $U=2\times 10^4$ cm sec^{-1},

$$\Delta T \approx 40\,\mathrm{K}/N$$

so that if the layer in which the temperature difference produced by the convection zone is, for example, ten scale heights deep, $\Delta T \approx 4$ K. This is within the error limits of equator – pole temperature difference observations made so far.

8. Needed Improvements for the Model

There are several major improvements needed in the model. In summary, these are: 1) spherical geometry; 2) compressibility; 3) more realistic boundary conditions, particularly at the top of the fluid region; 4) many more layers in the vertical and harmonics in the horizontal, or, alternatively, a three-dimensional grid for a spherical shell.

At present there is work in progress by others on a model for a spherical shell which still has two layers, but which has more harmonics in the horizontal. This model allows for a potential field outside the spherical shell that is solved for simultaneously with the dynamo field in the fluid. In our model, the annulus geometry gives us a differential rotation with a maximum in the middle of the annulus (i.e., mid-latitudes within one hemisphere on the sun) which is not particularly realistic. It is hoped that the spherical shell model will give an equatorial acceleration as well as reversing magnetic fields. With a spherical shell model, the heliostrophic assumption is also dropped, since Coriolis forces in the heliostrophic balance vanish at the equator. Therefore the Rossby number expansion is also abandoned.

Unfortunately, because of the computing expense, it will not be possible in the immediate future to test the convergence of models of our type when many more harmonics and layers are added.

In addition to the above improvements needed, we also need to know more about solar convection, particularly how big the eddy viscosity produced by it is, and how big a latitudinal temperature gradient it can produce when influenced by rotation.

Finally, we are also developing mathematical models to test the dynamo and differential rotation maintenance capabilities of giant convective cells on the sun arising from the vertical temperature gradient rather than a latitudinal one. These motions have one advantage over thermally driven Rossby waves in that modelling them requires fewer assumptions that have no direct observational support.

Acknowledgements

Dr. Martin Altschuler made useful comments on the manuscript. I am indebted to Mrs. Patricia Jones who programmed all computations, and Mrs. Maxine Shelton who typed the manuscript. Computations were performed on the CDC 6400 computer of the University of Colorado Graduate Computing Center. This research was sponsored in part by the Air Force Cambridge Research Laboratory, Office of Aerospace Research, under contract F19628-67-C-0304, but does not necessarily reflect endorsement by the sponsor.

References

Babcock, H. W.: 1961, *Astrophys. J.* **133**, 572.
Bumba, V. and Howard, R.: 1965, *Astrophys. J.* **141**, 1502.
Cocke, W. J.: 1967, *Astrophys. J.* **150**, 1041.
Gilman, P. A.: 1968, *Science* **160**, 760.
Kraichnan, R. H. and Nagarajan, S.: 1967, *Phys. Fluids* **10**, 859.
Leighton, R. B.: 1964, *Astrophys. J.* **140**, 1547.
Lilly, D.: 1965, *Monthly Weather Rev.* **93**, 11.
Lorenz, E. N.: 1962, *J. Atmospheric Sci.* **19**, 39.
Lorenz, E. N.: 1963, *Ibid.* **20**, 448.